Equatorial Waves in the Presence of Air–Sea Heat Exchange

HOWARD P. HANSON

Cooperative Institute for Research in Environmental Sciences, University of Colorado, Boulder 80309

(Manuscript received 1 December 1982, in final form 28 March 1983)

ABSTRACT

Changes in propagation of free linear waves on the equatorial β-plane associated with air–sea heat exchange are investigated here. By using a mixed-layer model, with the waves considered as perturbations on a specified basic state, the usual separability problems are avoided and the sea surface temperature is carried as a prognostic variable. The heat exchange is limited to that associated with turbulent fluxes, and a simplified air–sea transfer function allows analytic solutions of the various equatorial modes.

The problem is reduced to the classical solutions for a single vertical mode with the air–sea heat flux and mixed layer entrainment feedback effects cast in terms of three adjustment scales: an atmospheric adjustment length scale and two oceanic adjustment time scales, one for the response to surface fluxes and one for the response to entrainment. In order for the feedback to have any effect, both surface fluxes and entrainment must be included.

Propagation speeds of the equatorial waves are affected significantly by the presense of feedback. For an assumed easterly wind, the Kelvin wave speed is decreased by as much as 15% and the Rossby wave speeds are increased by as much as 50%, depending on the magnitude of the feedback parameters. In addition, the feedback increases (decreases) the wave-related SST amplitude for downwind (upwind) propagating waves over that for the no-feedback case. This is not a positive feedback, however, because the dissipative nature of the feedback causes the solutions to decay.

1. Introduction

The theory of linear waves on the equatorial β-plane has undergone substantial development in recent years as interest in these motions as a mechanism to explain the El Niño phenomenon has arisen and as the large oceanographic data sets generated by the GARP Atlantic Tropical Experiment and the Indian Ocean Experiment have stimulated theoreticians. The formal theory (e.g., Moore and Philander, 1977) has been restricted to studies of adiabatic motion, with no change in the upper ocean density structure forced by surface heat fluxes.[1] Despite this rather unphysical restriction, the theory has proved quite successful at describing the basic current structures in the equatorial oceans. For example, the El Niño phenomenon is described as the ocean's response to a relaxation of the Pacific trades after a period of relatively strong trade wind flow during which the east–west sea level gradient builds up. After the trades relax, an eastward propagating Kelvin wave suppresses the thermocline, which, by inference, is associated with surface warming. Upon reaching the South American coast the wave energy is reflected westward in Rossby waves and it also generates coastally-trapped Kelvin waves which propagate north and south (McCreary, 1976). That the linear theory is successful in describing this sequence of events has been demonstrated by Busalacchi and O'Brien (1980, 1981), whose numerical calculations of the linear theory with a reduced gravity model corresponding to the first baroclinic mode forced by actual wind records correlate quite well with observed sea level changes. Another example of the theory's usefulness is McCreary's (1981) model of the Equatorial Undercurrent. Although this model neglects (nonlinear) advective processes, which are undoubtedly important, it provides a sound basis for understanding the various regimes of equatorial dynamics. More recently Gill (1983) has shown that the advection of the mean temperature field by equatorial wave motions can account for much of the sea-surface temperature (SST) variability observed in the central Pacific.

This variability is thought to be an important aspect of climate variability through teleconnections with other parts of the earth. Webster's (1981) modeling shows that tropical SST anomalies can produce a larger response than midlatitude SST anomalies because the longer advective time scales in the tropical atmosphere (Webster's *diabatic limit*) allow initial heating anomalies to amplify through a positive diabatic–dynamic feedback. Hoskins and Karoly (1981) used a linear model to show the propagation

[1] Recently, Rothstein (1983) has relaxed this restriction and examined SST variations in response to wind-stress forcing in McCreary's (1981) model.

of low-latitude heating-induced planetary waves to midlatitudes through global wave guides, and recently Blackmon *et al.* (1983) have simulated this phenomenon using a low resolution general circulation model. Similar patterns have been discussed in the context of atmospheric data sets by Horel and Wallace (1981) and Wallace and Gutzler (1981). These teleconnection processes involve the diabatic response of the atmosphere to SST anomalies through latent-heat induced vertical motion, and it seems probable that the ocean is affected by the same diabatic interactions. The linear equatorial wave theory does not address this phenomenon directly because the SST is generally carried only as a passive scaling constant. The quantity predicted is the heat content (or pressure or upper layer thickness, all of which are proportional), and "warming events" are deduced in the theory on the basis of heat content changes. Interactive atmosphere–ocean models (e.g., Lau, 1981) have used the ocean's heat content as if it were the SST, to induce latent heat fluxes into the atmosphere. In the real ocean, of course, both the upper layer thickness and the SST vary; their relative phase may or may not produce the heat content variability seen in the linear models (e.g., Gill, 1982). That the calculations of Busalacchi and O'Brien (1980, 1981) reproduce sea level records suggests that the linear theory is indeed successful, but the mechanisms of the heat content variability in the ocean are not clear.

This research addresses the role of sea–air heat exchange in the traditional equatorial dynamics by examination of β-plane free wave solutions with the SST carried as a predictive (i.e., time dependent) variable. This is accomplished by using a linearized mixed-layer model, the basic state of which turns out to correspond approximately to the third baroclinic model. This paper is a follow-up study to a recent investigation by Kraus and Hanson (1983), who examined the propagation of SST anomalies in the presence of air–sea interaction processes with a non-rotational equatorial channel model. They found that air–sea heat exchange increased propagation rates in the linear model over the mean advective current speed by as much as a factor of 2. The mean current is ignored here in favor of the equatorial waves; notwithstanding, it is found that the heat exchange can enhance wave propagation rates by as much as 50%.

2. Model development

Motions on the equatorial β-plane are considered as wave perturbations on a steady basic state; basic state advection is ignored for simplicity but could be included (without shear) by using a Lagrangian transformation (e.g., Philander, 1979). The equations used here follow, with some notational changes, Eqs. (14) of Kraus and Hanson (1983) with the addition of meridional variability and with no basic state variability:

$$u'_t - \beta y v' + \eta'_x = 0, \tag{1a}$$

$$v'_t + \beta y u' + \eta'_y = 0, \tag{1b}$$

$$h'_t + h_0(u'_x + v'_y) - W'_E = 0, \tag{1c}$$

$$T'_t + h_0^{-1}[F' + (W_E T)'] = 0, \tag{1d}$$

$$(W_E \eta)' - \alpha g h_0 F' = 0. \tag{1e}$$

Here, subscript zero and the prime denote basic and perturbation quantities; α and g are the coefficient of thermal expansion and gravity; β is the gradient of the Coriolis parameter at the equator; h the mixed-layer depth and W_E the entrainment rate; u, v, x, y, t have their usual meanings and $\eta = \alpha g h T$ is a buoyancy variable proportional to the layer heat content where T is the mixed-layer temperature excess over the (constant) layer below. Here F is the (upward) heat flux at the surface and will be coupled to T below. Equations (1c) and (1d) are the vertically-integrated forms of mass continuity and heat conservation; Eq. (1e) is a simplified form of Niiler and Kraus' (1977) entrainment rate based on turbulent kinetic energy considerations. If wind stress perturbations were included, they would appear in (1e) as well as (1a) and (1b). Using the standard linearization that products of primed quantities be neglected, $\eta' = \alpha g(T_0 h' + h_0 T')$, etc.

By defining

$$F_* \equiv \alpha g F', \tag{2a}$$

$$T \equiv \frac{T'}{T_0}, \tag{2b}$$

$$h \equiv \frac{h'}{h_0}, \tag{2c}$$

$$\eta \equiv \frac{\eta'}{\eta_0}, \tag{2d}$$

and dropping the primes from u and v, (1a)–(1e) reduce to

$$u_t - \beta y v + \eta_0(T_x + h_x) = 0, \tag{3a}$$

$$v_t + \beta y u + \eta_0(T_y + h_y) = 0, \tag{3b}$$

$$h_t + \zeta_E h + u_x + v_y - \frac{F_*}{\eta_0} = 0, \tag{3c}$$

$$T_t - \zeta_E h + \frac{2F_*}{\eta_0} = 0, \tag{3d}$$

where the entrainment time scale for the basic state layer is $\zeta_E \equiv W_{E0}/h_0$. Eqs. (3c) and (3d) further combine to give

$$\eta_t + u_x + v_y + \frac{F_*}{\eta_0} = 0. \tag{3e}$$

The standard equatorial β-plane theory derives from (3a), (3b) and (3e) with $F_* = 0$ [note that, with Eqs. (2), $\eta' = \eta_0(T + h)$]. These equations then correspond to a baroclinic mode of equivalent depth $h_e = \eta_0/g$. The dispersion relation for the meridional Hermite structure is recovered as

$$\omega^2 - C_K^2 k\left(k + \frac{\beta}{\omega}\right) - C_K\beta(2m + 1) = 0, \qquad (4)$$

where $C_K = \sqrt{\eta_0}$ and $m = -1, 0, 1 \cdots$ yield, respectively, the Kelvin, Yanai (mixed), and gravity (Rossby- and inertia-) modes, C_K being the Kelvin wave speed. Fig. 1 shows the k–ω dispersion diagram for frequencies which will be significantly affected by the feedback; for the basic state used here, the lowest-frequency ($m = 1$) inertia–gravity wave occurs on Fig. 1 at $(\omega, k) \sim (8 \cdot 10^{-6}\ \mathrm{s}^{-1}; 0.14 \cdot 10^{-5}\ \mathrm{m}^{-1})$. Fig. 1 assumes an 8.4 cm equivalent depth; this is based on an 80 m mixed layer which is 3.5°C warmer than the layer below, values typical of the east-central equatorial Pacific (Halpern, 1980; Wyrtki and Edlin, 1982). This approximates the third baroclinic mode. For convenient reference, a semi-annual wave ($2\pi/\omega = 6$ months) occurs at $\omega \cong 0.4\ 10^{-6}\ \mathrm{s}^{-1}$.

In this paper, emphasis is placed on the behavior of waves in the equatorial ocean with and without air–sea heat exchange. A number of processes which are potentially important for SST anomaly evolution and propagation are therefore neglected in order to isolate the diabatic role of air–sea interaction; these include temperature changes in and below the thermocline, coupling across the mixed layer interface associated with shear stresses, advection by mean currents and waves and feedback to the wind stress. Furthermore, the ocean–atmosphere coupling is maintained in as simple a form as possible. This coupling is assumed to take the form of transfer function, such that the SST and the air–sea temperature difference are related according to

$$T' - \vartheta = fT', \qquad (5a)$$

where T' is the (dimensional) SST perturbation, ϑ is the associated atmospheric temperature perturbation and f is the sea–air transfer function, an explicit form of which will be derived below. It is also convenient to define a time scale ζ_S for the mixed layer's response to surface heat flux changes such that

$$\frac{F_*}{\eta_0} = \zeta_S fT. \qquad (5b)$$

Substituting for F_*/η_0, Eqs. (3) become:

$$u_t - \beta yv + \eta_0(T_x + h_x) = 0, \qquad (6a)$$

$$v_t + \beta yu + \eta_0(T_y + h_y) = 0, \qquad (6b)$$

$$h_t + \tau_E h + u_x + v_y - \zeta_S fT = 0, \qquad (6c)$$

$$T_t - \tau_E h + 2\zeta_S fT = 0, \qquad (6d)$$

and, combining (6c) and (6d),

$$\eta_t + u_x + v_y + \zeta_S fT = 0. \qquad (6e)$$

The two time scales of ζ_E and ζ_S will be seen below to play significant roles in the feedback. Physically, they represent the adjustment times of the basic state mixed layer to basic state entrainment and to heat flux perturbations, respectively. The layer's response to entrainment perturbations is built into Eqs. (6).

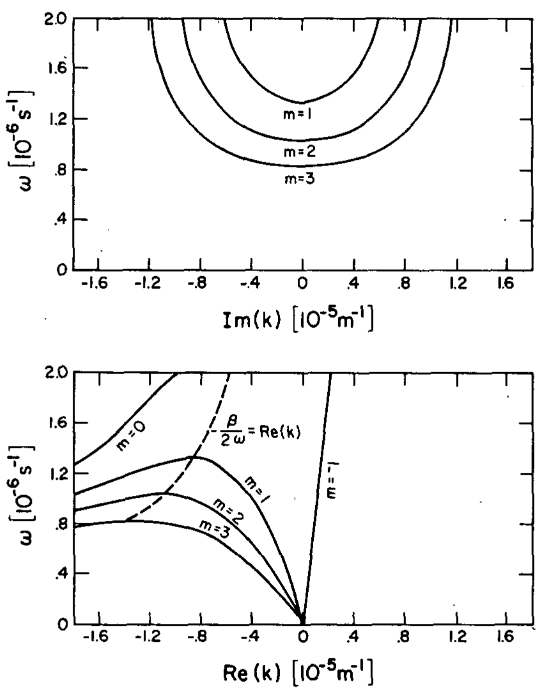

FIG. 1. Low-frequency part of equatorial β-plane dispersion diagram, showing Kelvin ($m = -1$), Yanai ($m = 0$) and Rossby ($m = 1, 2, 3$) modes (lower panel) and the $\mathrm{Im}[k(\omega)]$ transitions for ($m = 1, 2, 3$) when $\mathrm{Re}[k(\omega)] = -\beta/2\omega$ (upper panel).

3. Heat flux feedback results

a. The general solution

Since air–sea turbulent heat exchange depends on the SST, the four-equation set (6a–d) must be solved. It is useful, however, to examine the hypothetical case of a "heat content feedback," for which the substitution of η for T is made in Eq. (6e). Scaling y according to

$$y_F \equiv (1 + \Omega)^{1/4}\left(\frac{\beta}{C_K}\right)^{1/2} y, \qquad (7a)$$

where, in this case, $\Omega = i\zeta_s f/\omega$, leads to the canonical differential equation

$$\{\partial^2/\partial y_F^2 + [(2m + 1) - y_F^2]\}(v) = 0, \qquad (7b)$$

with waves dispersing according to (4) with C_K replaced by

$$C_F \equiv [1 + \Omega]^{-1/2} C_K. \tag{7c}$$

That the eigenvalues used in (7b) remain the same as in the no-feedback case is required by convergence of the power series solution to the boundary conditions $v \to 0$ as $y \to \pm\infty$. (That is, the usual Hermite functions are the only solutions which satisfy this boundary condition.) Another perspective on this can be gained from examination of the (Gaussian) weighting of the Hermite polynomials in the solutions, $\exp(-y_F^2/2)$. It can be shown that, for this to vanish as $y \to \pm\infty$, the inequality $\mathrm{Im}(\Omega) \geq 0$ must hold. For the inherently dissipative air–sea transfer function f used here, this is always the case, both for the "heat content" feedback and the SST feedback below.

Solving the SST feedback case is somewhat less straightforward. The simplest approach to Eqs. (6a–6d) appears to be to eliminate h using (6d) and to proceed to eliminate in favor of v in the usual manner. The necessary algebra results in the canonical structure (7) for

$$\Omega = \frac{-\zeta_S \zeta_E f/\omega}{\omega + i(\zeta_E + 2\zeta_S f)}. \tag{8}$$

This differs from the simpler, artificial case above with stronger frequency dependence and an additional phase shift (this is consistent with the increased complexity of four equations over three). Note that *both* surface heating and entrainment are necessary to have any effect on the dynamics, since if either ζ_S, $\zeta_E = 0$, $\Omega = 0$. The inclusion of feedback in this manner produces a very compact result that depends entirely on the modified Kelvin wave speed C_F. In particular, the feedback in this formulation can be examined for any air–sea transfer function f.

The velocity, temperature and mixed-layer depth fields follow from the usual forms, e.g., Moore and Philander (1977). Assume a complex amplitude A_m (m s^{-1}) for the mth horizontal mode of the meridional velocity such that

$$v_m(x, y, t) = \mathrm{Re}\{A_m \exp[i(kx - \omega t)]\psi_m(y_F)\}, \tag{9a}$$

where the (normalized) Hermite function ψ_m is

$$\psi_m(y_F) = \frac{(-1)^m}{(2^m m! \sqrt{\pi})^{1/2}} \exp\left(\frac{-y_F^2}{2}\right) H_m(y_F), \tag{9b}$$

with H_m the mth Hermite polynomial. Then the zonal velocity, heat content, mixed-layer depth and temperature are given by (the real parts being assumed):

$$u_m = iA_m \exp[i(kx - \omega t)](\beta C_F)^{1/2} \times \left\{\frac{m\psi_{m-1}}{\omega + C_F k} + \frac{\psi_{m+1}}{2(\omega - C_F k)}\right\}, \tag{10a}$$

$$\eta_m = -iA_m \exp[i(kx - \omega t)]\left(\frac{C_F^2}{\eta_0}\right)\left(\frac{\beta}{C_F}\right)^{1/2} \times \left\{\frac{m\psi_{m-1}}{\omega + C_F k} - \frac{\psi_{m+1}}{2(\omega - C_F k)}\right\}, \tag{10b}$$

$$h_m = \eta_m(1 + \Omega) \times \left\{\frac{\omega(\omega + 2_i\zeta_S f)}{\omega[\omega + i(\zeta_E + 2\zeta_S f)] - \zeta_E\zeta_S f}\right\}, \tag{10c}$$

$$T_m = \eta_m(1 + \Omega) \times \left\{\frac{i\omega\zeta_E}{\omega[\omega + i(\zeta_E + 2\zeta_S f)] - \zeta_E\zeta_S f}\right\}. \tag{10d}$$

Note $\eta_m = h_m + T_m$. Eqs. (9), (10a) and (10b) also hold for the "heat content feedback."

The system of equations (6) has not been scaled, but rather solved in dimensional, unscaled form in order to elucidate the roles of the feedback adjustments. The factor $(\beta C_F)^{1/2}$ appearing in (10a) is an inverse time scale; the factor $(\beta/C_F)^{1/2}$ in (10b) is an inverse length scale. (In the undisturbed state, these are $\sim$(2.6 day)$^{-1}$ and $\sim$(200 km)$^{-1}$, respectively, for the basic state used here.) These are the natural scales for the system under consideration [see, e.g., Eq. (7a)]. The velocity scale with feedback is thus C_F (Moore and Philander, 1977); in particular, C_F scales the Rossby wave speeds. This wave speed, then, serves as a useful tool to examine the effects of feedback on the system as a whole.

b. *The sea–air transfer function*

Equatorial wave theory in a reduced-gravity-type model has been extended above to include SST variability and heat exchange with the atmosphere. In order to see how these processes affect the propagation of the waves, it is necessary to introduce an explicit form for the sea–air transfer function f. In this paper, the approach of Kraus and Hanson (1983) is adopted for reasons of simplicity and in order to isolate the ocean as a dynamic system. This approach neglects changes in the atmospheric circulation and radiation and focuses attention on the effects of changes in atmospheric temperatures. Interactive atmosphere–ocean models, such as that of Lau (1981) include changes in the atmospheric circulation; such models therefore are associated not only with (a more complicated form of) the thermodynamic transfer function f used here, but would also imply a dynamic transfer function, associated with circulation changes, between SST changes and changes in the large-scale wind stress patterns. The latter is ignored in this paper. Atmospheric radiation at the sea surface is strongly affected by the cloud field, which is coupled to the lower-atmosphere stability and circulation. A cloud model is far beyond the scope of this paper, and changes in the radiative fluxes at the sea surface are neglected here in favor of the turbulent fluxes.

Since the thermal inertia of the ocean is so much larger than that of the atmosphere, changes in time of atmospheric heat storage are neglected. Rather, the atmosphere is presumed to adjust to changes in ocean temperature over some distance λ^{-1} along the trades. This can be written as

$$\vartheta_x = \lambda(T' - \vartheta), \tag{11}$$

where ϑ is the atmospheric temperature response and T' is the (dimensional) SST perturbation. By identifying the left side with zonal advection and the right with atmospheric heating in a layer of depth H_A due to the surface fluxes, λ can be estimated as

$$\lambda \sim \frac{C_D}{H_A}\frac{|U_A|}{U_A}\left(1 + \frac{1}{B_0}\right), \tag{12}$$

where the drag coefficient ($C_D \sim 1.5 \times 10^{-3}$) and wind speed ($|U_A|$) are associated with the bulk formula, and the Bowen ratio (B_0) is to be interpreted here as the latent heat flux which contributes locally to condensation heating within the depth H_A. Limits on λ can be inferred by considering two (rather nonphysical) cases: if H_A is the sub-cloud layer depth ($\sim$500 m) and all the latent heat is released in this layer (ignoring the contradiction) then $\lambda \sim (25\ \text{km})^{-1}$; if the entire tropical troposphere is heated by the sensible heat flux alone (so that all the moisture is presumed to be advected away), then $\lambda \sim (10^4\ \text{km})^{-1}$. Kraus and Hanson varied λ between (10^2 and 10^3 km)$^{-1}$; here attention is focused on two values, $\lambda = (200\ \text{km})^{-1}$; $(500\ \text{km})^{-1}$. For an atmospheric advective rate $U_A = 5$ m s^{-1}, this implies atmospheric adjustment time scales of $\sim$0.5 and 1.2 days, respectively. These represent *thermodynamic* adjustment times and are reasonable values for the lower tropical atmosphere (e.g., Houze and Betts, 1981).

Wave solutions to (11) then yield the form of the transfer function used in the following section:

$$f = \frac{k}{k - i\lambda}. \tag{13}$$

Note that (12) implies that λ is not necessarily positive, due to the wind speed in the numerator and the wind velocity in the denominator. Since the wavenumber k can be of either sign (the convention that $\omega > 0$ and real is used here), the sign of λ is an important part of the feedback, as is seen in the results below.

c. Numerical examples

Without feedback effects, the ($m = -1$) Kelvin wave is non-dispersive; in the present case $C_K \approx 0.908$ m s^{-1}. The feedback causes the Kelvin wave to become dispersive [cf., Eq. (7c)]. Fig. 2 shows the behavior of the Re(C_F) for the Kelvin wave subject to a variety of atmospheric and oceanic adjustment scales. (The values $\lambda > 0$ imply westerly winds.) Also shown are the Rossby wave cutoffs (i.e., where Re(k) $= -\beta/2\omega$ for m = 1, 2 on Fig. 1). The effects of the air–sea feedback are confined to low frequencies and indicate the enhancement of the wave speed when it propagates downwind. The greatest enhancement occurs at the lowest frequencies and, for the $\lambda = (500\ \text{km})^{-1}$; $\zeta_S \approx (23\ \text{days})^{-1}$ (i.e., curves 2 and 7) cases represents an $\sim$15% increase in wave speed. This is rather a fast response time for the ocean; at longer oceanic adjustment scales (smaller ζ_S) the effect is smaller. For the implied cases of easterly winds, ($\lambda < 0$), the Kelvin wave speed is decreased.

The coupled atmosphere–ocean models which set atmospheric heating proportional to the ocean heat content have, thus far, not investigated the immediate heat flux feedback to the ocean, as above. One might therefore ask, how would they behave if that were done? This can be examined by looking at the variations in C_F if the "heat content feedback" is used (i.e., $\Omega = i\zeta_S f/\omega$). Such a calculation is shown in Fig. 3 for some of the cases in Fig. 2. (ζ_E does not enter the problem here). Although the qualitative behavior in Fig. 2 is reproduced–largest response at lowest frequencies and downwind propagation enhancement—this artificial case exhibits a significant response at much higher frequencies than the SST feedback. The

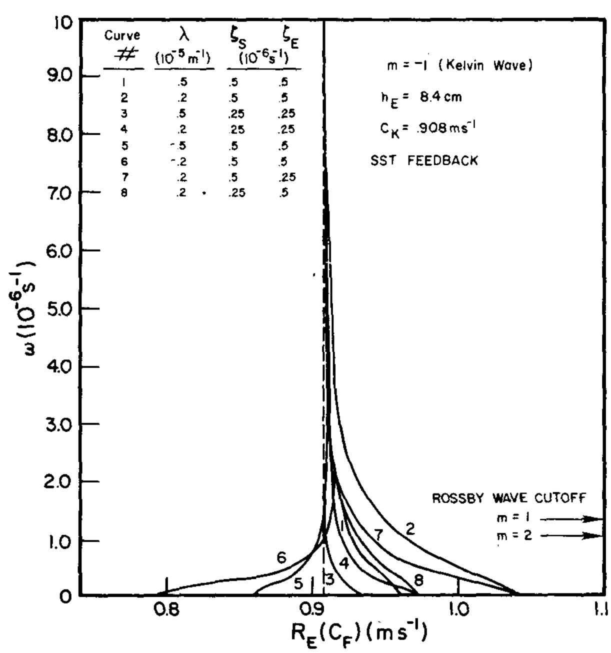

FIG. 2. Kelvin wave speeds for various combinations of SST feedback parameters, no feedback (short dashes).

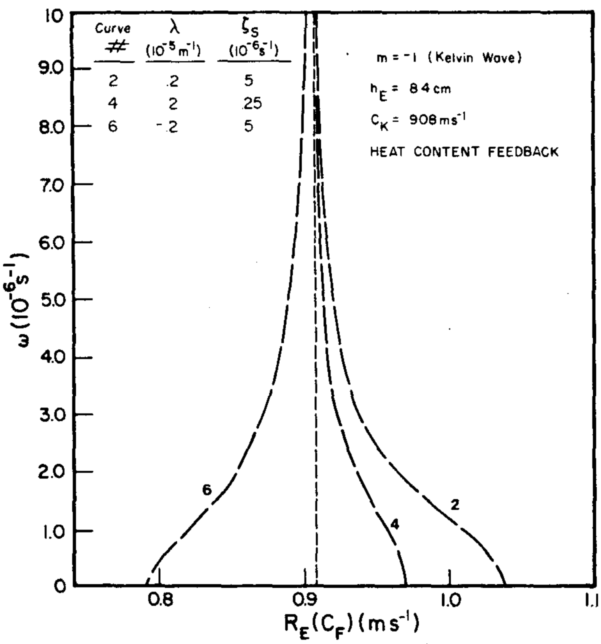

FIG. 3. As in Fig. 2 for the "heat-content feedback."

physical mechanism for this will be made clear in the discussion below.

The Rossby waves respond to the feedback in the same physical sense as the Kelvin wave. Fig. 4 shows the $m = 1$ Rossby wave phase speeds; the short dashes in the quasi-parabola represent ω/k from Fig. 1 (no feedback), the long dashes the heat content feedback and the solid curves the SST feedback. Since the Rossby waves propagate westward, their speed is enhanced by easterly winds ($\lambda < 0$) and retarded by westerlies. Note that the response is greater here; as much as 50% enhancement is observed for the case analogous to that which yielded a 15% enhancement of the Kelvin wave. The phase speed of the six-month wave, when added to a mean current of about -0.3 m s^{-1}, gives a westward propagation rate of approximately -0.7 m s^{-1}. This is within the range of 0.5–1.0 m s^{-1} inferred by Rasmusson and Carpenter (1982) from a composite of Pacific warming events.

The mechanism responsible for this enhanced westward propagation can be illuminated further by examination of the heat flux associated with the waves, $\overline{u\eta} = \overline{uT} + \overline{uh}$. This is facilitated by the forms chosen for $v(x, y, t)$ in Eqs. (9) and for u and η in Eqs. (10). Fig. 5a shows the magnitude of T, h, η for the SST feedback (solid) and η for the heat content feedback (long dashes) all normalized by the magnitude of η for no feedback. The difference between the two types of feedback is similar to that discussed for the Kelvin and Rossby wave speeds, i.e., the SST feedback produces a lower response at the higher frequencies than does the artificial heat content feedback. The flair of both η curves near $\omega = 1.3 \times 10^{-6}$ s^{-1} is due to the no-feedback response becoming very small. This is more apparent in Fig. 5b, where the fluxes are proportional to the group velocity, which vanishes at the cutoff frequency around $\omega = 1.33 \times 10^{-6}$ s^{-1}.

This increased magnitude of the heat content (or SST) associated with the waves can be interpreted physically as a pumping mechanism of the waves by the air–sea heat exchange as follows. Considering the simplest case—the heat content feedback and the Kelvin wave—leads to

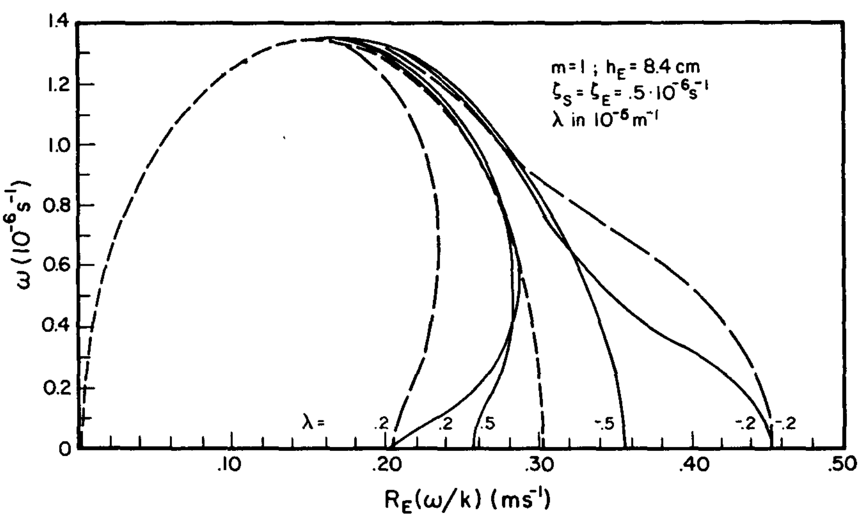

FIG. 4. Rossby wave speed for $m = 1$; no feedback (short dashes), heat-content feedback (long dashes), SST feedback (solid lines).

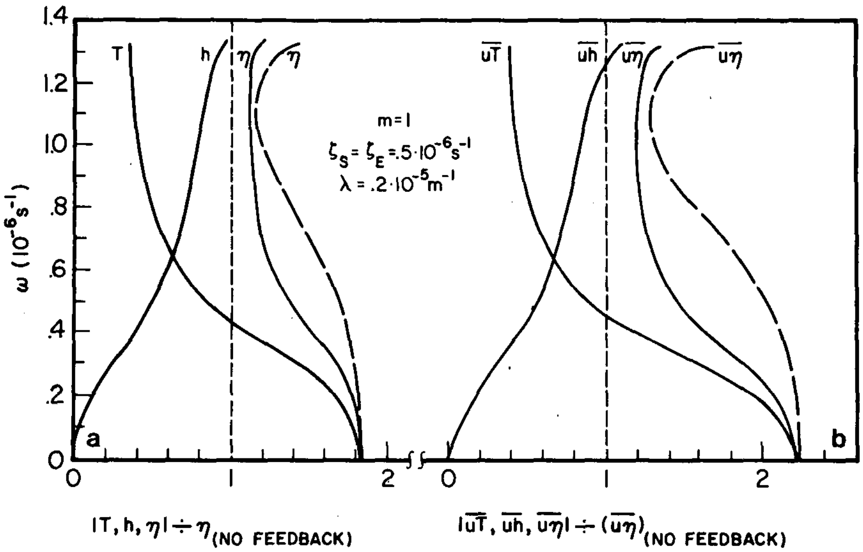

FIG. 5. (a) magnitudes of mixed layer depth h, temperature T, and heat content η, normalized by the no-feedback case. Heat content feedback is shown by the long dashed line. (b) As in (a), but for zonal fluxes.

$$u_t + \eta_x = 0, \quad (14a)$$

$$\eta_t + a\eta + \eta_0 u_x = 0, \quad (14b)$$

where the coefficient a is now complex (it takes the place of $\zeta_s f$ in (6e) for this discussion). In terms of the wave amplitude U, the heat content is $\omega/k \times \{U \exp[i(kx - \omega t)]\}$ and the dispersion relation gives $\omega/k = \eta_0^{1/2}(1 + ia/\omega)^{-1/2}$. If a is real and positive, the middle term in (14b) is simply a Newtonian cooling term and the solution decays. If a is pure imaginary and positive, this term plays a role analogous to a (negative) imaginary index of refraction in radiative transfer theory—i.e., an emission coefficient—and the amplitude of the solution is increased. In all cases here, $\mathrm{Re}(a) \propto \mathrm{Re}(f) > 0$ and the waves decay in space, while for downwind (upwind) propagating waves $\mathrm{Im}(a) \propto \mathrm{Im}(f) > (<)0$ and amplitudes are enhanced (retarded). The form of the amplification factor $(1 + ia/\omega)^{-1/2}$ shows that the lowest frequencies are most strongly affected.

This discussion also applies to the more general SST feedback case. Note, however, that Fig. 5 shows the response of this more complex case to occur in two distinct regimes. At lower frequencies, a thermal response, with large SST variability, dominates, while at higher frequencies, a mechanical response begins to assume control, with the mixed layer depth variability becoming larger. The thermal regime is associated with the enhanced propagation speeds shown in Fig. 4. It should be noted that models that carry the SST as a scaling factor implicitly operate only in the mechanical regime.

4. Discussion

The mixed layer formulation used here is, of course, a highly idealized simplification of the equatorial Pacific. In the three-dimensional problem, a mixed layer can be included but it projects on to several baroclinic modes (McCreary, 1981). In a reduced-gravity approach, such as Busalacchi and O'Brien's (1980) numerical model, it is not necessary to assume the upper layer to be well mixed, as only the integrated heat content is predicted. The connection between the present approach and these models is two-fold. First, the mixed-layer model reduces to the usual shallow water equations when feedback is excluded [cf., Eqs. (6)] and the consequent identical physics provide a useful basis for discussing the cases with variable SST. Second, the mixed-layer model includes a vertical coupling (due to the basic state entrainment term ζ_E and the built-in entrainment perturbations) which varies inversely with the basic state layer depth; this is closely analogous to the form used by McCreary (1981) in which higher-order baroclinic modes are more strongly vertically coupled. In the present model, ζ_E acts as a Rayleigh damping term. Its neglect in the momentum equations therefore overestimates the decay scale of the solutions; it does not, however, affect the enhanced feedback response discussed above because it has no imaginary counterpart of the surface term $\zeta_S f$.

The disparity between the SST feedback and the artificial "heat content" feedback noted in the previous section concerns the over-response of the latter in the 4-month, or so, frequency range. It can be inferred from Fig. 2 that this difference is controlled by the vertical coupling term ζ_E. For example, curves 2 and 7 differ only in that ζ_E is halved in curve 7; this confines the model response to lower frequencies. In fact, comparing the forms of Ω for the two types of feedback shows that the "heat-content" feedback is the limit of the SST feedback as $\zeta_E \to \infty$. The heat content feedback is therefore simply a very-strongly-coupled limit of the true physical situation; this, of course, merely restates the mathematical derivations in physical terms.

It must be noted that the projection of the wind stress forcing is stronger for low-order modes (Moore and Philander, 1977) and that the initial Kelvin wave following a decrease in the strength of the trades is likely to be a first-mode response, at least in the central Equatorial Pacific. The present model results, indicating a retarded third-mode (approximately) Kelvin wave due to air–sea heat exchange are likely not observable. Moreover, the air–sea interaction considered here is implicitly much less efficient at modifying the lower order modes since both ζ_E and ζ_S are inversely proportional to the basic state layer depth. As seen in Fig. 2, low values of these (inverse) adjustment times imply little modification of the wave speed.

5. Conclusion

Using a mixed-layer model with a simplified entrainment formulation on the equatorial beta plane, the role of air–sea heat exchange in the propagation of free equatorial waves is examined. The basic state layer, on which the waves are considered perturbations, is chosen to be relevant to the east-central Equatorial Pacific with a Kelvin wave speed of 0.908 $m\ s^{-1}$. A simple form of air–sea interaction, for which the SST and the sea–air temperature difference are assumed to be related by a complex transfer function is studied. The equatorial wave solutions are cast in the canonical forms by definition of a feedback parameter (Ω_F); this modifies both the equatorial trapping scale and the velocity scale, making both frequency-dependent.

The sea–air transfer function is formulated in a very simple fashion, by neglecting radiation and considering that the atmosphere adjusts to SST changes over some (prescribed) distance. Results show that wave propagation speeds in the downwind (upwind) direction are enhanced (retarded). If the speed of the feedback enhanced $m = 1$ Rossby wave is added to that of the mean surface current, the resulting westward propagation rate is strikingly similar to that observed for warming events in the Equatorial Pacific and to that for the first baroclinic mode. In association with the changes in wave speeds, the feedback increases (decreases) the magnitude of the wave-related SST. This "pumping" mechanism can be interpreted as a negative imaginary refractive index for the waves and is most effective at very-low frequencies. Notwithstanding the increased amplitudes, the inherently dissipative nature of the feedback, which takes the form of a Rayleigh damping in this linear problem, causes the waves to decay.

It is important to stress that this model is not meant to simulate the complete dynamics of the Equatorial Pacific, since only free wave solutions have been examined, and since the wind stress projects strongly onto lower order baroclinic modes. This study has shown the potential importance, previously neglected, of diabatic air–sea interaction processes in the dynamics of the equatorial oceans.

Acknowledgments. This paper is dedicated to the memory of Walter O. Düing. Discussions with Eric Kraus have been most helpful in clarifying the topics of air–sea interaction studied here, and Claus Rooth and Don Olson provided useful comments on the paper. This research was supported by National Science Foundation Grant ATM-80-23334 and by the National Oceanic and Atmospheric Administration through the Equatorial Pacific Ocean Climate Studies program.

REFERENCES

Blackmon, M. L., J. E. Geisler and E. J. Pitcher, 1983: A general circulation model study of January climate anomaly patterns associated with interannual variation of equatorial Pacific sea surface temperatures. *J. Atmos. Sci.*, **40**, 580–604.

Busalacchi, A. J., and J. J. O'Brien, 1980: The seasonal variability in a model of the tropical Pacific. *J. Phys. Oceanogr.*, **10**, 1929–1951.

——, and ——, 1981: Interannual variability of the equatorial Pacific in the 1960's. *J. Geophys. Res.*, **86**, 10 901–10 907.

Gill, A. E., 1982: Changes in the thermal structure of the equatorial Pacific during the 1972 El Niño as revealed by bathythermograph observations. *J. Phys. Oceanogr.*, **12**, 1373–1387.

——, 1983: An estimation of sea-level and surface-current anomalies during the 1972 El Niño and consequent thermal effects. *J. Phys. Oceanogr.*, **13**, 586–606.

Halpern, D., 1980: A Pacific equatorial temperature section from 170°E to 110°W during winter–spring 1979. *Deep Sea Res.*, **27**, 931–940.

Horel, J. D., and J. M. Wallace, 1981: Planetary-scale atmosphere phenomena associated with the Southern Oscillation. *Mon. Wea. Rev.*, **109**, 813–829.

Hoskins, B. J., and D. J. Karoly, 1981: The steady linear response of a spherical atmosphere to thermal and orographic forcing. *J. Atmos. Sci.*, **31**, 1179–1196.

Houze, R. A., Jr., and A. K. Betts, 1981: Convection in GATE. *Rev. Geophys. Space Phys.*, **19**, 541–576.

Kraus, E. B., and H. P. Hanson, 1983: Air–sea interaction as a propagator of equatorial ocean surface temperature anomalies. *J. Phys. Oceanogr.*, **13**, 130–138.

Lau, K-M, 1981: Oscillations in a simple equatorial climate system. *J. Atmos. Sci.*, **38**, 248–261.

McCreary, J., 1976: Eastern tropical ocean response to changing wind systems: with application to El Niño. *J. Phys. Oceanogr.*, **6**, 632–645.

——, 1981: A linear stratified ocean model of the Equatorial Undercurrent. *Phil. Trans. Roy. Soc. London,* **A298,** 603–635.

Moore, D. W., and S. G. H. Philander, 1977: Modeling of the tropical oceanic circulation. *The Sea,* Vol. 6, Wiley Interscience, 319–361.

Niiler, P. P., and E. B. Kraus, 1977: One-dimensional models of the upper ocean. *Modelling and Prediction of the Upper Layers of the Ocean,* Pergamon, 143–172.

Philander, S. G. H., 1979: Equatorial waves in the presence of the Equatorial Undercurrent. *J. Phys. Oceanogr.,* **9,** 254–262.

Rasmusson, E. M., and T. H. Carpenter, 1982: Variations in tropical sea surface temperature and surface wind fields associated with the Southern Oscillation/El Niño. *Mon. Wea. Rev.,* **110,** 354–384.

Rothstein, L., 1983: A model of the equatorial SST field and circulation dynamics. Ph.D. dissertation, University of Hawaii.

Wallace, J. M., and D. S. Gutzler, 1981: Teleconnection in the geopotential height field during the Northern Hemisphere winter. *Mon. Wea. Rev.,* **109,** 813–829.

Webster, P. J., 1981: Mechanisms determining the atmospheric response to sea surface temperature anomalies. *J. Atmos. Sci.,* **38,** 554–571.

Wyrtki, K., and G. Edlin, 1982: Equatorial upwelling events in the central Pacific. *J. Phys. Oceanogr.,* **12,** 984–988.